European Journal of Medicinal Chemistry 110 (2016) 291–301

Contents lists available at ScienceDirect

European Journal of Medicinal Chemistry

journal homepage: http://www.elsevier.com/locate/ejmech

Research paper

5-Substituted 3-isopropyl-7-[4-(2-pyridyl)benzyl]amino-1(2)*H*-pyrazolo[4,3-*d*]pyrimidines with anti-proliferative activity as potent and selective inhibitors of cyclin-dependent kinases

Ladislava Vymětalová [a], Libor Havlíček [b], Antonín Šturc [a], Zuzana Skrášková [a], Radek Jorda [a], Tomáš Pospíšil [a], Miroslav Strnad [a], Vladimír Kryštof [a, *]

[a] Laboratory of Growth Regulators, Centre of the Region Haná for Biotechnological and Agricultural Research, Palacký University and Institute of Experimental Botany AS CR, Šlechtitelů 27, 78371 Olomouc, Czech Republic
[b] Isotope Laboratory, Institute of Experimental Botany ASCR, Vídeňská 1083, 14220 Prague, Czech Republic

ARTICLE INFO

Article history:
Received 7 October 2015
Received in revised form
8 January 2016
Accepted 9 January 2016
Available online 18 January 2016

Keywords:
Cyclin-dependent kinase
Inhibitor
Selectivity
Bioisostere

ABSTRACT

A series of 5-substituted 3-isopropyl-7-[4-(2-pyridyl)benzyl]amino-1(2)*H*-pyrazolo[4,3-*d*]pyrimidine derivatives was synthesized and evaluated for their cyclin-dependent kinase (CDK) inhibition activity. The most potent compounds contained various hydroxyalkylamines at the 5 position and possessed low nanomolar IC_{50} values for CDK2 and CDK5. Preliminary profiling of one of the most active compounds on a panel of 50 protein kinases revealed its high selectivity for CDKs. The compounds arrested cells in S and G2/M phases, and induced apoptosis in various cancer cell lines. Significant dephosphorylation of the C-terminus of RNA polymerase II and focal adhesion kinase (FAK), well-established substrates of CDKs, has been found in treated cells. Cleavage of PARP-1, down-regulation of Mcl-1 and activation of caspases correlated well with CDK inhibition and confirmed apoptosis as the primary type of cell death induced in cancer cells treated with the compounds *in vitro*. A comparison of known purine-based CDK inhibitor CR8 with its pyrazolo[4,3-*d*]pyrimidine bioisosteres confirmed that the novel compounds are more potent in cellular assays than purines. Therefore, pyrazolo[4,3-*d*]pyrimidine may emerge as a novel scaffold in medicinal chemistry and as a source of potent CDK inhibitors.

1. Introduction

Deregulation of the cell cycle is a common hallmark of cancers and, on the molecular level, is tightly linked to cyclin-dependent kinases (CDKs). Upon binding to regulatory subunits called cyclins, these enzymes play a key role in the cell cycle, from initiation, through DNA replication, to mitosis [1]. Deregulation of CDKs is often caused by amplification or overexpression of cyclins, or by mutation or silencing of the genes encoding natural protein inhibitors of CDKs. In principle, however, many various upstream alterations can hyperactivate CDKs inappropriately and, as a consequence, promote proliferation of cancer cells despite the lack of mitogens [2]. Besides that, deregulation of CDKs induces genomic and chromosomal instability that mediate neoplastic transformation of cells [2].

Such observations in the vast majority of cancers provided a rationale for targeting CDKs using pharmacological inhibitors. The first small molecule CDK inhibitors, such as flavopiridol, roscovitine, and many others, demonstrated anti-proliferative and anti-cancer activity mediated by suppression of the expected targets. These targets comprised several CDK-family members including CDK1, CDK2, CDK4, CDK7, and CDK9 [3,4]. Both roscovitine and flavopiridol were therefore selected for clinical trials as anti-cancer drugs with a novel mechanism of action. However, both drugs exhibited toxicity and low efficacy. More potent compounds were developed soon afterward, and several were investigated in Phase II-III clinical trials [2].

Despite high sequence similarity within the CDK family, several truly monospecific CDK inhibitors were also identified, including CDK4-specific palbociclib [5], CDK7-specific irreversible binder THZ-1 [6], and CDK9-specific LDC000067 [7] (Fig. 1). Although it has proven necessary to inhibit several CDKs to produce anti-cancer activity in certain models, the abovementioned

Abbreviations: CDK, cyclin-dependent kinase; FAK, focal adhesion kinase.

* Corresponding author.
E-mail address: vladimir.krystof@upol.cz (V. Kryštof).

http://dx.doi.org/10.1016/j.ejmech.2016.01.011
0223-5234/

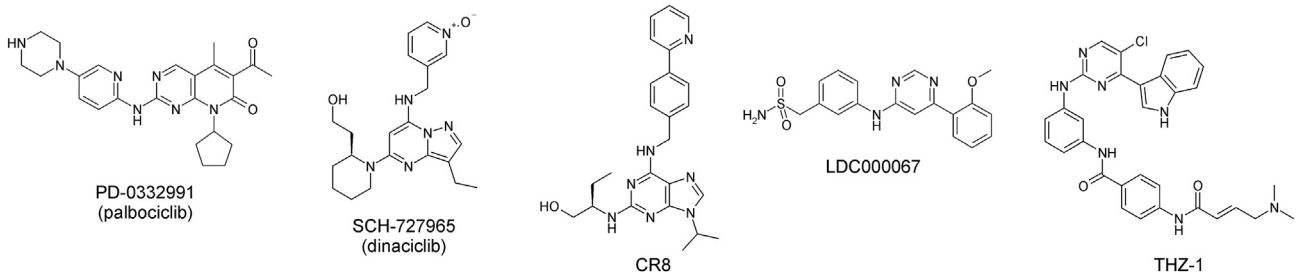

Fig. 1. Examples of known CDK inhibitors with varying selectivities.

palbociclib, with its higher selectivity for CDK4 and CDK6 than other CDKs, received accelerated FDA approval as the first compound in its class [8]. Palbociclib has shown efficacy in the treatment of certain breast cancers [9,10], but it becomes clear that other cancers will require different CDK selectivity patterns. Therefore, there is still a need for the development of new inhibitors.

We recently focused on the skeleton of pyrazolo[4,3-*d*]pyrimidine, an isostere of purine, and prepared a series of compounds substituted analogous to the purine-based roscovitine. To date, several other CDK inhibitors built on heterocycles isosteric to purine have been described (reviewed by Ref. [11]), but among them, only pyrazolo[1,5-*a*]pyrimidines, pyrazolo[1,5-*a*]-1,3,5-triazines, and pyrazolo[4,3-*d*]pyrimidines exceed the activity of corresponding purines. Compounds based on the latter group, the pyrazolo[4,3-*d*]pyrimidines, display anti-cancer activity [12,13]. In addition, some derivatives suppress abnormal proliferation related to the pathogenesis of restenosis in vascular smooth muscle cells [14] and tumor angiogenesis [15], all by inhibiting CDKs and aurora A kinase [13].

The objective of this work was to synthesize novel potent CDK inhibitors with a pyrazolo[4,3-*d*]pyrimidine scaffold bearing N6-biaryl substituents. N6-biaryl substituents were proven most advantageous for the activities of analogous purines, such as CR8, BP14, and others [16–19]. As we expected, the newly prepared derivatives displayed nanomolar potency against CDKs and cancer cell lines. The most potent derivative was over 7 times more active against CDK2 than CR8, and was comparable to another bioisostere of roscovitine, dinaciclib [20].

2. Results and discussion

2.1. Synthesis

The pyrazolo[4,3-*d*]pyrimidine substitutions were based on studies of structure-activity relationships for related purine and pyrazolo [1,5-*a*]pyrimidine CDK inhibitors, and included one of the most beneficial biarylamino substituents at position 7, *i.e.* [(2-pyridyl)benzyl]amine. Position 5 was modified using various side chains in order to understand the importance of each chain for activity. Products of position 5 modifications were also compared to the disubstituted derivative 3-isopropyl-7-[4-(2-pyridyl)benzyl] amino-1(2)H-pyrazolo[4,3-*d*]pyrimidine (**6**) that was prepared by reacting 7-chloro-3-isopropyl-1(2)H-pyrazolo[4,3-*d*]pyrimidine [21] with 1-[4-(pyridin-2-yl)phenyl]methanamine. Another simple derivative, 3-isopropyl-5-methylsulfanyl-7-[4-(2-pyridyl)benzyl] amino-1(2)H-pyrazolo[4,3-*d*]pyrimidine (**2a**) was prepared from 7-chloro-3-isopropyl-5-methylsulfanyl-1(2)H-pyrazolo[4,3-*d*]pyrimidine (**2**) by reaction with 1-[4-(pyridin-2-yl)phenyl]methanamine.

The synthesis of 5-substituted 3-isopropyl-7-[4-(2-pyridyl) benzyl]amino-1(2)H-pyrazolo[4,3-*d*]pyrimidines (Scheme 1) was based on two subsequent nucleophilic substitutions. This synthesis is analogous to the synthesis of the pyrazolo[4,3-*d*]pyrimidine bioisostere of roscovitine [12]. However, contrary to the synthesis of the roscovitine analog, oxidation of the methylsulfanyl group of compound **2** must be performed before nucleophilic substitution of the chloro atom at position 7 in order to prevent oxidation of the pyridylbenzylamine part of the desired product. Substitution of the chloro atom of compound **3** proceeds under gentle conditions (60 °C/1 h) in a high yield. Subsequent substitution of the methylsulfonyl group of compound **4** needs severe conditions (125—150 °C/5—30 h) producing approximately 20% yield of derivatives 5, which must be isolated by chromatography.

The structures of all newly-synthesized compounds were verified using NMR spectroscopy, ESI mass spectrometry, and elemental analysis. The purity of each synthesized compound was checked by HPLC-DAD analysis. Detailed information about synthesis and characterization of all compounds is described in the experimental and supporting information sections of this manuscript.

2.2. CDK inhibitory activity of novel pyrazolo [4,3-d]pyrimidines

The presence of a heterobiaryl substituent at position 6 of the purine molecule was proven crucial for CDK inhibitory activity, compared to monoaryl substituted derivatives like roscovitine [16,18,19]. This was clearly demonstrated by compound CR8 which showed a 3-fold lower IC_{50} for CDK2, and >200-fold higher potency in cells than roscovitine [16].

We synthesized a collection of 3,5,7-trisubstituted pyrazolo[4,3-*d*]pyrimidines with the same substitutions at positions 3 and 7 as CDK inhibitor CR8 and a different substitution at position 5. All novel derivatives were tested for CDK2/CDK5 kinase inhibition according to established protocols (see details in the Experimental section) and the data obtained are presented in Table 1.

The results demonstrate that most of the new compounds display significantly higher potency for inhibiting CDK2/CDK5 than the reference purine compound CR8, with IC_{50} values well below 100 nM. The 3,7-disubstituted pyrazolo[4,3-*d*]pyrimidine **6**, lacking substitution at position 5, was slightly more active than CR8, suggesting that the biaryl function at 7 markedly increases affinity of the skeleton to a CDK. Addition of a suitable substitution at position 5 further increased potency. A small increase in potency of inhibition of either CDK2 or CDK5 (IC_{50} values in a high nanomolar range) was observed when the scaffold was substituted, at position 5, with small sulphur-containing functions (**2a**, **4**). However the structures of most beneficial pyrazolo[4,3-*d*]pyrimidines with 5-substitutions, in terms of CDK inhibition, shared a hydroxyalkylamine or an aminoalkylamine motif (**5a**–**e**). This finding corresponds to earlier observations performed with analogous purine and pyrazolo[1,5-*a*] triazine inhibitors [18,19,22–24]. The most potent derivative, **5c**, showed IC_{50} values for CDK2 and CDK5 of 9 nM and 1 nM, respectively. The activity of **5c** is comparable to clinically developed

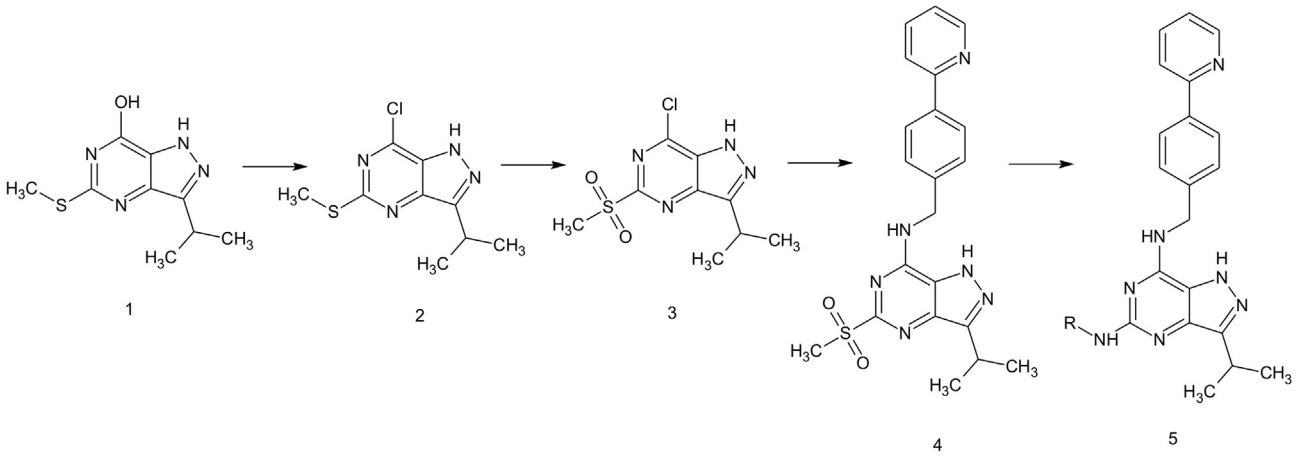

Scheme 1. Preparation of 3,5,7-trisubstituted pyrazolo[4,3-*d*]pyrimidines.

dinaciclib [20]. Only two newly-prepared derivatives, **5p** and **5q**, with aromatic chains at position 5, showed insufficient activity ($IC_{50} > 1$ μM). One study shows that the aromatic substitution at 5 is detrimental for the activity of related purine inhibitors [23].

We also compared one of the most active compounds, **5b**, with several other known CDK inhibitors: pan-selective dinaciclib, CDK7-specific BS-181, and CDK4-specific palbociclib (Table 2). Compound **5b** displayed a similar profile and potency to those of dinaciclib, with a slightly lower potency against CDK1. Preliminary selectivity profiling of **5b** was then performed using a panel of 50 additional protein kinases. The compound was assayed at a single concentration of 1 μM. As shown in the Supplementary Table S1, residual activity of other tested kinases reached values of approximately 50% (for CAMKKb) or 60% (for DYRK1A, CK1δ, AMPK, PAK4), which clearly confirmed **5b** selectivity (intrapolated residual activities of CDK2 and CDK5 are <10%). It was not surprising that **5b** also inhibited PAK4 or CK1δ because these kinases are sensitive to previously described pyrazolo[4,3-*d*]pyrimidines [13,14] and structurally related purines [16,25].

2.3. Activity in cancer cell lines

All novel derivatives were tested for cytotoxicity on four cancer cell lines (Table 1). Our data showed that the presence of substituents at position 5 rapidly increased cellular potency to nanomolar activities, compared to 3,7-disubstituted derivative **6**. While compound **6** displayed an IC_{50} of approximately 1 μM for all cancer cell lines, other derivatives showed mid-level (**5f**-**h**, **5j**-**k**, **5m**-**o**) or low (**5a**-**e**, **5l**) nanomolar IC_{50} values. These activities clearly correspond with anti-CDK activity. All derivatives with high cytotoxicity also displayed high affinity for CDK2 and vice versa, whereas derivatives **5p** and **5q** were significantly less active in both assays. Surprisingly, replacing hydroxyalkylamines with cyclic amines usually weakens cellular potency (IC_{50} values of **5f**-**h**, **5j**, **5n**, **5o** > 100 nM), although CDK inhibition in biochemical assays still occurred at a low nanomolar range. The most potent pyrazolo[4,3-*d*]pyrimidines, **5a**-**c** and **5l**, each showed an IC_{50} that was at least 10-fold lower than that of CR8.

Next, the activity of **5b**, one of the most potent inhibitors in the series of compounds, was studied in detail in a colon carcinoma cell line, HCT-116. As shown in Fig. 2A, treatment with 125 nM and higher concentrations of **5b** substantially decreased the S-phase population (BrdU-positive cells) of cells, increased the subG1 population (apoptotic cells), and arrested cells in late S and G2/M phases. In addition, similar effects were observed in breast adenocarcinoma cells, MCF-7, treated with **5b** and other pyrazolo[4,3-*d*]pyrimidines, compared to cells treated with CR8 (the control; Fig. S1). These results indicate that the compounds block DNA replication and proliferation in a dose-dependent manner, an effect attributable to CDK2 inhibition. Similar outcomes have been described for numerous other CDK inhibitors, such as roscovitine, dinaciclib, SNS032, and flavopiridol [20,26–28].

Due to structural similarities between CDK2 and CDK5, it was no surprise that the compounds inhibited both kinases (Table 1). Because CDK5 emerged as a new potential target of cancer therapy, we attempted to show that compound **5b** also targets CDK5 in cells. We immunoblotted lysates of treated HCT-116 cells and discovered a dose-dependent decrease of FAK phosphorylation at Ser 732 (Fig. 2B), which is a known CDK5 substrate [29,30].

Due to the strong cytotoxicity of **5b** in the HCT-116 cell line, we sought to identify the type of cell death that occurs, using biochemical assays. Lysates of treated HCT-116 cells were subjected to immunoblotting. Subsequent analysis revealed a dose-dependent decrease of anti-apoptotic protein Mcl-1 as well as cleavage of PARP-1, a known caspase substrate (Fig. 3A). We also found that **5b** rapidly increased the expression of tumor suppressor p53 at concentrations of 250 nM and higher. In addition, caspase activation in treated cells was confirmed by an enzymatic assay, using fluorescently labeled substrates of caspases 3 and 7 (Fig. 3B) that revealed clear dose-dependent responses in a sub-micromolar range.

Although CDK2 is dispensable for the growth of most tumors [31], some articles showed that CDK2 might be a suitable target for molecular therapy of primary and metastatic melanoma [32]. Indeed, the anti-melanoma activity of CDK inhibitors dinaciclib and roscovitine has been confirmed [33–35]. We therefore studied the effects of novel derivatives in a melanoma cancer cell line, G361. The tested derivatives potently activated caspases in treated cells (Supplemental Fig. S2). Moreover, ongoing apoptosis (as evidenced by immunoblotting of cleaved PARP-1 and decreased Mcl−1 levels) correlated well with reduced phosphorylation of RNA polymerase II at the C-terminus (Supplemental Fig. S3 and S4). Importantly, the tested derivatives induced cancer cell death in substantially lower doses than related purine derivative CR8 and pyrazolo[4,3-*d*]pyrimidine bioisostere of roscovitine (designated as compound 7) [12].

3. Conclusion

A library of 20 novel pyrazolo[4,3-*d*]pyrimidine derivatives,

Table 1
Cytotoxicity and anti-CDK activity of novel 3,5,7-trisubstituted pyrazolo[4,3-*d*]pyrimidines.

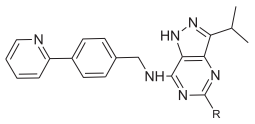

Compound	R	IC_{50}, (μM) Cancer cell lines K-562	MCF-7	G361	HCT-116	Kinases CDK2	CDK5
Roscovitine	n.a.	45.5	12.25	22.4	14.42	0.158	1.069
CR8	n.a.	0.175	0.160	0.503	0.350	0.062	0.225
6		1.000	1.190	0.875	1.237	0.197	0.183
2a		0.778	0.819	1.400	2.800	0.048	0.229
4		0.640	0.460	0.793	1.140	0.070	0.165
5a	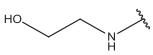	0.038	0.051	0.039	0.027	0.031	0.049
5b	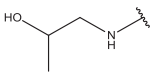	0.057	0.027	0.040	0.087	0.021	0.005
5c	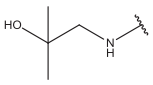	0.029	0.024	0.048	0.085	0.009	0.001
5d	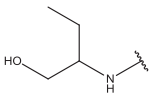	0.070	0.053	0.067	0.110	0.054	0.009
5e	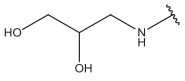	0.047	0.059	0.072	0.087	0.012	0.021
5f	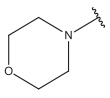	0.110	0.163	0.197	0.270	0.018	0.005
5g	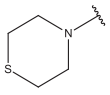	0.589	0.530	0.873	0.940	0.061	0.114
5h	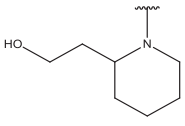	0.165	0.133	0.204	0.142	0.024	0.037
5i	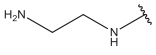	0.063	0.062	0.230	0.227	0.018	0.008
5j	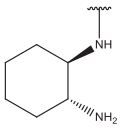	0.175	0.295	0.477	0.427	0.046	0.044
5k	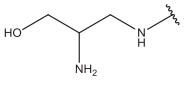	0.700	0.310	1.018	0.781	0.051	0.017
5l	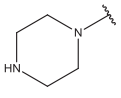	0.017	0.021	0.064	0.088	0.050	0.119
5m	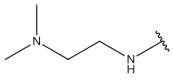	0.125	0.225	0.640	0.390	0.467	2.136

Table 1 (*continued*)

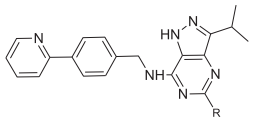

Compound	R	IC$_{50}$, (μM) Cancer cell lines K-562	MCF-7	G361	HCT-116	Kinases CDK2	CDK5
5n	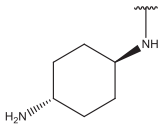	0.593	0.474	0.745	0.720	0.096	0.179
5o	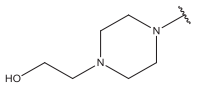	0.145	0.195	0.181	0.350	0.132	0.422
5p	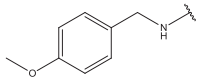	3.950	5.300	7.487	17.40	1.483	4.415
5q	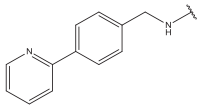	2.535	2.385	3.610	7.325	1.450	3.600

Table 2
CDK selectivity profile of Compound **5b** and some known CDK inhibitors (assayed as controls).

Kinases	IC$_{50}$ (μM)[a]			
	Cmpd. **5b**	Dinaciclib	BS-181	Palbociclib
CDK1	0.777	0.072	14.0	>10
CDK2	0.021	0.002	1.80	9.20
CDK4	>2	0.127	44.7	0.016
CDK5	0.034	0.045	3.70	>10
CDK7	2.780	n.a.	0.134	>10
CDK9	0.240	0.178	2.18	0.892

[a] Average values from at least three determinations.

with nanomolar inhibitory activities against CDK2 and CDK5, was generated. The majority of compounds demonstrated strong anti-proliferative effects, including cell cycle arrest and induction of apoptosis, for which CDK inhibition is a primary mode of action. Although the pyrazolo[4,3-*d*]pyrimidine is isosteric to purine and pyrazolo[1,5-*a*]pyrimidine and the new compounds are analogous to roscovitine and dinaciclib, we found that pyrazolo[4,3-*d*]pyrimidines were substantially more active than purines. This scaffold may serve as an alternative source of novel, potent CDK inhibitors that may display different physico-chemical and pharmacological properties. Therefore, pyrazolo[4,3-*d*]pyrimidine may emerge as a novel scaffold in medicinal chemistry and is worth further investigation, especially in the field of cancer therapeutics, where drug resistance significantly complicates efficacy.

4. Experimental section

4.1. Chemistry

NMR spectra were recorded on a JEOL ECA-500 spectrometer operating at frequencies of 500.16 MHz (^{1}H) and 125.76 MHz (^{13}C). ^{1}H NMR and ^{13}C NMR chemical shifts were referenced to the solvent signals; ^{1}H: δ(residual $CHCl_3$) = 7.25 ppm, δ(residual DMSO-

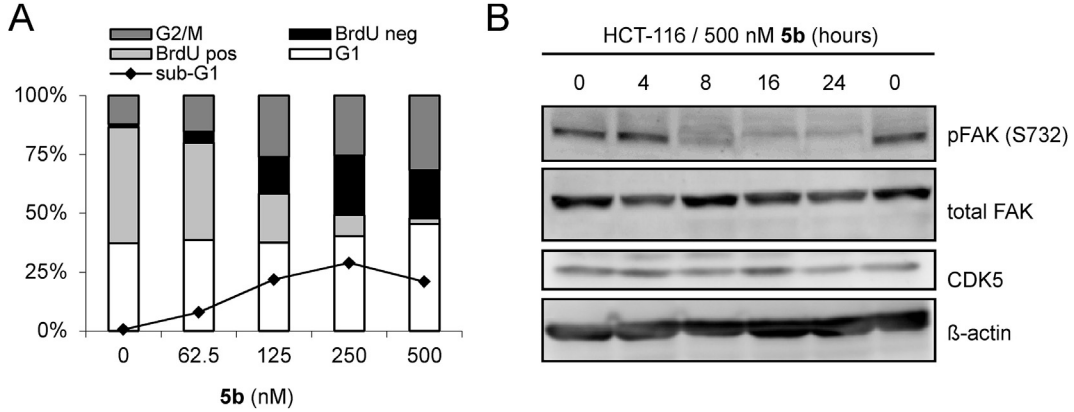

Fig. 2. Effect of 5b on the HCT-116 cancer cell line. (A) Asynchronous cells were treated with different concentrations of **5b** for 24 h. The cell cycle was analyzed by flow cytometry; DNA was double-labeled with propidium iodide and 5-bromo-2′-deoxyuridine. (B) Time-course immunoblotting analysis of phosphorylation of FAK, a known CDK5 substrate, in cells treated with 500 nM of **5b**. β-actin was detected to verify equal loading.

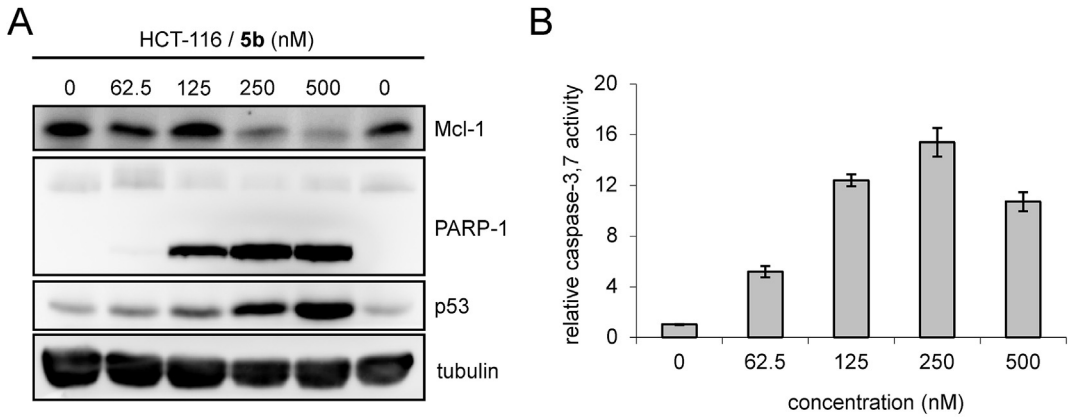

Fig. 3. Induction of apoptosis in HCT-116 cancer cells treated with different doses of **5b** for 24 h. (A) Immunoblotting analysis of apoptosis-related proteins in treated cells. Tubulin levels were detected to verify equal loading. (B) Fluorimetric assay for caspase-3 and caspase-7 activity in lysates prepared from treated cells. Caspase activity was measured using the fluorogenic substrate Ac-DEVD-AMC and normalized against untreated control cell lysates.

d_5) = 2.50 ppm, δ(residual CD_2HOD) = 3.31 ppm; ^{13}C: $\delta(CDCl_3)$ = 77.23 ppm, δ(DMSO-d_6) = 39.52 ppm, $\delta(CD_3OD)$ = 49.15 ppm. Chemical shifts are given in δ scale [ppm] and coupling constants in Hz.

Melting points were determined on a Kofler block and are uncorrected. Reagents were of analytical grade and from standard commercial sources. Thin layer chromatography (TLC) was carried out using aluminium sheets with silica gel F_{254} from Merck. Spots were visualized under UV light (254 nm). ESI mass spectra were determined using a Waters Micromass ZMD mass spectrometer (solution in MeOH, direct inlet, coin voltage 20 V). Column chromatography was performed using Merck silica gel Kieselgel 60 (230–400 mesh). The purity of all synthesized compounds was determined by HPLC-PDA (200–500 nm). Specific optical rotation was measured on polarimeter polAAr 3001 (wave length: 589.44 nm, tube length: 5 cm, and t = 23 °C). All compounds gave satisfactory elemental analyses (0.4%).

4.1.1. 3-Isopropyl-5-methylsulfanyl-1(2)H-pyrazolo[4,3-d] pyrimidin-7-ol (**1**)

This compound was prepared as previously described [12].

4.1.2. 7-Chloro-3-isopropyl-5-methylsulfanyl-1(2)H-pyrazolo[4,3-d]pyrimidine (**2**)

This compound was prepared as previously described [12].

4.1.3. 3-Isopropyl-5-methylsulfanyl-7-[4-(2-pyridyl)benzyl]amino-1(2)H-pyrazolo[4,3-d]pyrimidine (**2a**)

A solution of 7-Chloro-3-isopropyl-5-methylsulfanyl-1(2)H-pyrazolo[4,3-*d*]pyrimidine (**2**) (0.56 g, 2.3 mmol), 1-[4-(pyridin-2-yl)phenyl]methanamine (0.48 g, 2.6 mmol) and ethyldiisopropylamine (0.86 mL, 5 mmol) in 12 mL t-BuOH was heated with stirring at 70 °C for 2 h. After cooling to room temperature, the reaction mixture was concentrated under vacuum and the residue was partitioned between H_2O and $CHCl_3$. The combined organic phase was dried with magnesim sulfate and evaporated. Crystallization from $CHCl_3/Et_2O$ generated a colorless product with m.p. = 170–173 °C, mass = 0.79 g, and 87% yield. ESI + *m/z* 391.1 $[M+H]^+$, ESI- *m/z* 389.1 $[M-H]^-$. ^1H (500 MHz; DMSO-d_6): 1.36 (d, *J* = 7.03 Hz, 6H, $-CH(CH_3)_2$); 2.43 (s, 3H, $-SCH_3$); 3.31–3.35 (m, 1H, $-CH(CH_3)_2$); 4.75 (bs, 2H, $-NH-CH_2-$); 7.32 (ddd, *J* = 7.34 Hz, *J* = 4.89 Hz, *J* = 0.92 Hz, 1H, ArH); 7.48 (d, *J* = 7.03 Hz, 2H, ArH); 7.84 (dt, *J* = 7.64 Hz, *J* = 1.53 Hz, 1H, ArH); 7.92 (d, *J* = 7.95 Hz, 1H, ArH); 8.05 (bd, *J* = 7.03 Hz, 2H, ArH); 8.63 (bd, *J* = 4.58 Hz, 1H, ArH). Anal. ($C_{21}H_{22}N_6S$) C, H, N, S.

4.1.4. 7-Chloro-3-isopropyl-5-methylsulfonyl-1(2)H-pyrazolo[4,3-d]pyrimidine (**3**)

Oxone^R solution (monopersulfate comp., Aldrich Cat: 228036, 36 g) in water (180 mL) was added in a dropwise manner, within 1 h, to a solution of 7-chloro-3-isopropyl-5-methylsulfanyl-1(2)H-pyrazolo[4,3-*d*]pyrimidine (**2**) (10 g, 41.3 mmol) in EtOH (180 mL) at 55 °C. The reaction mixture was stirred for another hour at 60 °C. After cooling to room temperature, the EtOH was removed by evaporation and the residue was partitioned between H_2O and EtOAc. The combined organic phase was dried with sodium sulfate. Crystallization from $EtOAc/Et_2O$ generated a product with m.p. = 111–114 °C, mass = 9.17 g, and 81% yield. ESI- *m/z* 273.1 $[M-H]^-$. ^1H NMR ($CDCl_3$): 1.49 (d, J = 6.96, 6H, $CH(CH_3)_2$); 3.49 (s, 3H, CH_3), 3.58 (sep, J = 6.96, 1H, CH). Anal. ($C_9H_{11}ClN_4O_2S$) C, H, N, S.

4.1.5. 3-Isopropyl-5-methylsulfonyl-7-[4-(2-pyridyl)benzyl]amino-1(2)H-pyrazolo[4,3-d]pyrimidine (**4**)

A mixture of 7-Chloro-3-isopropyl-5-methylsulfonyl-1(2)H-pyrazolo[4,3-*d*]pyrimidine (**3**) (4.89 g, 17.8 mmol) and ethyldiisopropylamine (4 mL, 22.5 mmol) were heated with stirring in 80 mL t-BuOH at 60 °C. A solution of 1-[4-(pyridin-2-yl)phenyl] methanamine (3.84 g, 20.9 mmol) in 30 mL t-BuOH (50 °C) was added and the reaction mixture was heated at 60 °C for 1 h. The product started to crystallize after 10 min. After cooling at room temperature, the product was filtered off, washed with MeOH and dried under vacuum; the product had m.p. = 214–218 °C, mass = 6.4 g, and 85% yield. ESI + *m/z* 423.3 $[M+H]^+$, ESI- *m/z* 421.3 $[M-H]^-$.^1H (500 MHz; DMSO-d_6): 1.38 (d, *J* = 6.72 Hz, 6H, $-CH(CH_3)_2$); 3.27 (s, 3H, CH3); 3.31–3.35 (m, 1H, $-CH(CH_3)_2$); 4.82 (bs, 2H, $NH-CH_2-$); 7.30–7.32 (m, 1H, ArH); 7.53 (d, *J* = 7.00 Hz, 2H, ArH); 7.82–7.86 (m, 1H, ArH); 7.91–7.92 (m, 1H, ArH); 8.05 (bs, 2H, ArH); 8.63 (bd, *J* = 4.28 Hz, 1H, ArH). Anal. ($C_{21}H_{22}N_6O_2S$) C, H, N, S.

4.1.6. 3-Isopropyl-5-(2-hydroxyethyl)amino-7-[4-(2-pyridyl) benzyl]amino-1(2)H-pyrazolo[4,3-d]pyrimidine (**5a**)

A solution consisting of 3-isopropyl-5-methylsulfonyl-7-[4-(2-pyridyl)benzyl]amino-1(2)H-pyrazolo[4,3-*d*]pyrimidine (**4**) (0.20 g, 0.48 mmol) and ethanolamine (4 mL, 66 mmol) was heated in a sealed ampoule at 130 °C for 25 h. Excess amine was evaporated at a temperature below 70 °C, and the residue was partitioned between H_2O and $CHCl_3$. The combined organic phase was dried with sodium sulfate and evaporated under vacuum. The product was purified by column chromatography: stepwise (5%, 6%, 8%, 10%) with MeOH in $CHCl_3$ containing a trace of concentrated aqueous

NH_4OH. Chromatography provided (after evaporation under vacuum) a noncrystalizable, amorphous colorless glass foam, with mass = 0.10 g, and 51% yield. ESI + *m/z* 404.1 $[M+H]^+$, ESI- *m/z* 402.1 $[M-H]^-$. ^1H (500 MHz; $CDCl_3$): 1.18 (d, *J* = 7.07 Hz, 6H, $-CH(CH_3)_2$); 3.09 (sept., *J* = 7.03 Hz, 1H, $-CH(CH_3)_2$); 3.41 (bs, 2H, $-CH_2-$); 3.69 (bs, 2H, $-CH_2-$); 4.57 (bs, 2H, $-NH-CH_2-$); 7.12 (qd, *J* = 7.64 Hz, *J* = 4.89 Hz, *J* = 1.22 Hz, 1H, ArH); 7.21 (d, *J* = 7.95 Hz, 2H, ArH); 7.52 (d, *J* = 7.95 Hz,1H, ArH); 7.62 (td, *J* = 7.34 Hz, *J* = 1.83 Hz, 1H, ArH); 7.72 (d, *J* = 7.95 Hz,1H, ArH); 8.54 (d, *J* = 4.58 Hz, 1H, ArH). ^{13}C (125 MHz; $CDCl_3$): 21.4, 25.9, 43.9, 45.3, 64.3, 120.6, 122.1, 127.0, 127.8, 136.9, 138.1, 138.8, 149.3, 152.3, 156.8, 158.2. Anal. ($C_{22}H_{25}N_7O$) C, H, N.

4.1.7. 3-Isopropyl-5(R)-(2-hydroxypropyl)amino-7-[4-(2-pyridyl) benzyl]amino-1(2)H-pyrazolo[4,3-d]pyrimidine (**5b**)

A solution consisting of 3-isopropyl-5-methylsulfonyl-7-[4-(2-pyridyl)benzyl]amino-1(2)H-pyrazolo[4,3-*d*]pyrimidine (**4**) (1.25 g, 2.96 mmol) in R-(−)-1-amino-2-propanol (10 mL, 110 mmol) in a sealed ampoule was heated at 130 °C for 12 h. Excess amine was evaporated at a temperature below 60 °C, and the residue was partitioned between H_2O and $CHCl_3$. The combined organic phase was dried with sodium sulfate and evaporated under vacuum. The product was purified by column chromatography, stepwise (3%, 5%, 7%) with MeOH in $CHCl_3$ containing a trace of concentrated aqueous NH_4OH. Chromatography provided (after evaporation under vacuum) a noncrystalizable, amorphous colorless glass form, with mass = 0.65 g, and 52% yield. ESI + *m/z* 418.1 (100%) $[M+H]^+$, 209.6 (20%) $[M+2H]^{2+}$, ESI- *m/z* 416.1 $[M-H]^-$. ^1H (500 MHz; DMSO-d_6 + $CDCl_3$): 0.99 (d, *J* = 6.42 Hz, 3H, $-CH_3$); 1.27 (d, *J* = 7.03 Hz, 6H, $-CH(CH_3)_2$); 3.06–3.11 (m, 2H, $-CH_2-$); 3.20–3.23 (m, 1H, $-CH(CH_3)_2$); 3.72–3.75 (m, 1H, −CH−); 4.69 (bs, 2H, $-NH-CH_2-$); 6.02 (bs, 1H, $-NH-CH_2-$); 7.27–7.30 (m, 1H, ArH); 7.45 (d, *J* = 7.34 Hz, 2H, ArH); 7.63 (bs, 1H, −NH−); 7.82 (dt, *J* = 7.64 Hz, *J* = 1.53 Hz, 1H, ArH); 7.88–7.89 (m, 1H, ArH); 8.01 (s, 2H, ArH); 8.60 (d, *J* = 3.97 Hz, 1H, ArH); 11.76 (bs, 1H, -NH-). ^{13}C (125 MHz; DMSO-d_6 + $CDCl_3$): 21.9, 22.2, 26.6, 43.4, 49.9, 66.7, 120.5, 122.8, 127.2, 128.4, 137.7, 149.8, 156.3. Anal. ($C_{23}H_{27}N_7O$) C, H, N. $[\alpha]_D$ = + 2.6° (MeOH, c = 5 mg/mL, 23 °C).

4.1.8. 3-Isopropyl-5-(2-hydroxy-2-methylpropyl)amino-7-[4-(2-pyridyl)benzyl]amino-1(2)H-pyrazolo[4,3-d]pyrimidine (**5c**)

A mixture of 3-isopropyl-5-methylsulfonyl-7-[4-(2-pyridyl) benzyl]amino-1(2)H-pyrazolo[4,3-*d*]pyrimidine (**4**) (0.6 g, 1.42 mmol) and 1-amino-2-methyl-2-propanol (1.25 g, 14 mmol) was heated at 150 °C for 15 h in a sealed ampoule. After cooling, the reaction mixture was partitioned between H_2O and $CHCl_3$. The combined organic phase was dried with sodium sulfate and evaporated under vacuum. The product was purified by column chromatography, stepwise (3%, 5%, 7%) with MeOH in $CHCl_3$. Chromatography provided (after evaporation under vacuum) a noncrystalizable, amorphous colorless glass form, with 0.2 g, and 33% yield. ESI + *m/z* 432.1 $[M+H]^+$, ES- *m/z* 430.1 $[M-H]^-$. ^1H (500 MHz; DMSO-d_6): 1.06 (s, 6H, $(OH)C(CH_3)_2$); 1.29 (d, *J* = 7.03 Hz, 6H, $-CH(CH_3)_2$); 3.14 (sept., *J* = 7.03 Hz, 1H, $-CH(CH_3)_2$); 3.20 (d, *J* = 5.81 Hz, 2H, $-NH-CH_2-$); 4.73 (d, *J* = 4.89 Hz, 2H, $-NH-CH_2-$); 6.12 (bs, 1H, $-NH-CH_2-$); 7.31 (dd, *J* = 7.03 Hz, *J* = 5.50 Hz, 1H, ArH); 7.48 (d, *J* = 7.95 Hz, 2H, ArH); 7.84 (dt, *J* = 7.64 Hz, J = 1.53 Hz, 1H, ArH); 7.91 (d, *J* = 7.95 Hz, 1H, ArH); 8.04 (d, *J* = 7.64 Hz, 2H, ArH); 8.63 (d, *J* = 4.28 Hz, 1H, ArH). Anal. ($C_{24}H_{29}N_7O$) C, H, N.

4.1.9. 3-Isopropyl-5(R)-[1-(hydroxymethyl)propyl]amino-7-[4-(2-pyridyl)benzyl]amino-1(2)H-pyrazolo[4,3-d]pyrimidine (**5d**)

A solution of 3-isopropyl-5-methylsulfonyl-7-[4-(2-pyridyl) benzyl]amino-1(2)H-pyrazolo[4,3-*d*]pyrimidine (**4**) (0.5 g, 1.19 mmol) in R-(−)-2-amino-1-butanol (5 mL, 50 mmol) was heated at 150 °C for 15 h in a sealed ampoule. Excess amine was evaporated at a temperature below 70 °C, and the residue was partitioned between H_2O and $CHCl_3$. The combined organic phase was dried with sodium sulfate and evaporated under vacuum. The product was purified by column chromatography, stepwise (3%, 5%, 7%) with MeOH in $CHCl_3$. Chromatography provided (after evaporation under vacuum) a noncrystalizable, amorphous colorless glass form, with mass = 0.14 g, and 27% yield. ESI + *m/z* 432.1 $[M+H]^+$, ESI- *m/z* 430.1 $[M-H]^-$. ^1H (500 MHz; DMSO-d_6): 0.81 (t, *J* = 6.72 Hz, 3H, $-CH_2-CH_3$); 1.39–1.45 (m, 7H, $-CH(CH_3)_2$, $-CH\alpha-CH_3$); 1.55–1.59 (m, 1H, $-CH\beta-CH_3$); 3.43–3.47 (m, 1H, $-CH(CH_3)_2$); 3.77–3.80 (m, 1H, −CH-NH−); 4.49–4.67 (m, 4H, $-CH_2-OH$, $-NH-CH_2-$); 5.82 (d, J = 7.64 Hz, 1H, $-NH-CH_2-$); 7.29–7.31 (m, 1H, ArH); 7.44 (d, *J* = 7.95 Hz, 2H, ArH); 7.78 (s, 1H, NH); 7.83 (t, *J* = 8.01 Hz, 1H, ArH); 7.89 (d, *J* = 7.95 Hz, 1H, ArH); 7.99 (d, *J* = 8.25 Hz, 2H, ArH); 8.62 (bd, *J* = 4.58 Hz, 1H, ArH. Anal. ($C_{24}H_{29}N_7O$) C, H, N. $[\alpha]_D$ = + 45.5° (MeOH, c = 1.9 mg/mL, 23 °C).

4.1.10. 3-Isopropyl-5-(2,3-dihydroxypropyl)amino-7-[4-(2-pyridyl) benzyl]amino-1(2)H-pyrazolo[4,3-d]pyrimidine (**5e**)

A mixture of 3-isopropyl-5-methylsulfonyl-7-[4-(2-pyridyl) benzylamino]-1(2)H-pyrazolo[4,3-*d*]pyrimidine (**4**) (0.20 g, 0.47 mmol), and 2,3-dihydroxypropylamine (2 mL, 26 mmol) was heated at 125 °C for 20 h. After cooling to room temperature, the reaction mixture was partitioned between H_2O and $CHCl_3$. The combined organic phase was dried with sodium sulfate and evaporated under vacuum. The product was purified by column chromatography, stepwise (3%, 5%, 8%, and 10%) with MeOH in $CHCl_3$. Chromatography provided (after evaporation under vacuum) a noncrystalizable, amorphous colorless glass form, with mass = 0.05 g, and 25% yield. ESI + *m/z* 434.1 $[M+H]^+$, ESI- *m/z* 432.1 $[M-H]^-$. ^1H (500 MHz; DMSO-d_6): 1.29 (d, *J* = 6.72 Hz, 6H, $-CH(CH_3)_2$); 1.85–1.91 (m, 1H, $-CH_\alpha H_\beta-$); 2.16 (t, *J* = 8.25 Hz, 1H, $-CH_\alpha H_\beta-$); 3.14–3.16 (m, 1H, $-CH(CH_3)_2$); 3.20–3.34 (m, 2H, $-CH_2-$); 3.54–3.56 (m, 1H, −CH−); 4.72 (bs, 2H, $-NH-CH_2-$); 6.18 (bs, 1H, −NH−); 7.32 (dd, *J* = 6.72 Hz, *J* = 5.50 Hz, 1H, ArH); 7.48 (d, *J* = 7.34 Hz, 2H, ArH); 7.85 (td, *J* = 7.79 Hz, *J* = 1.83 Hz, 1H, ArH); 7.91 (d, *J* = 7.95 Hz, 1H, ArH); 8.03 (bs, 2H, ArH); 8.63 (d, *J* = 3.97 Hz, 1H, ArH); 11.85 (bs, 1H, -NH-). ^{13}C (125 MHz; DMSO-d_6): 17.2, 21.7, 30.2, 42.7, 44.8, 48.5, 63.5, 71.9, 120.2, 122.5, 126.6, 128.0, 137.3, 149.6, 155.8. Anal. ($C_{23}H_{27}N_7O_2$) C, H, N.

4.1.11. 3-Isopropyl-5-(N-morpholinyl)-7-[4-(2-pyridyl)benzyl] amino-1(2)H-pyrazolo[4,3-d]pyrimidine (**5f**)

A mixture of 3-isopropyl-5-methylsulfonyl-7-[4-(2-pyridyl) benzyl]amino-1(2)H-pyrazolo[4,3-*d*]pyrimidine (**4**) (0.36 g, 0.85 mmol) and morpholine (3 mL, 27 mmol) in a sealed ampoule was heated at 150 °C for 8 h. Excess morpholine was evaporated at a temperature below 70 °C, and the residue was partitioned between H_2O and $CHCl_3$. The combined organic phase was dried with sodium sulfate and evaporated under vacuum. The product was purified by column chromatography, stepwise (2%, 4%, 5%) with MeOH in $CHCl_3$. Chromatography provided (after evaporation under vacuum) a noncrystalizable, amorphous colorless glass foam, with mass = 0.15 g, and 41% yield. ESI + *m/z* 430.1 $[M+H]^+$, ES- *m/z* 428.1 $[M-H]^-$. ^1H (500 MHz; DMSO-d_6): 1.32 (d, J = 7.03 Hz, 6H, $-CH(CH_3)_2$); 3.18 (bs, 1H, $-CH(CH_3)_2$); 3.58–3.60 (bs, 8H, 4×$-CH_2-$); 4.74 (bs, 2H, $-NH-CH_2-$); 7.31 (dd, *J* = 6.72 Hz, *J* = 5.50 Hz, 1H, ArH); 7.48 (d, *J* = 7.95 Hz, 2H, ArH); 7.78 (bs, 1H, −NH−); 7.84 (dt, *J* = 7.64 Hz, *J* = 1.53 Hz, 1H, ArH); 7.91 (d, *J* = 7.95 Hz, 1H, ArH); 8.04 (d, *J* = 5.81 Hz, 2H, ArH); 8.63 (d, *J* = 3.97 Hz, 1H, ArH); 11.84 (bs, 1H, −NH−). Anal. ($C_{24}H_{27}N_7O$) C, H, N.

*4.1.12. 3-Isopropyl-5-(thiomorpholinyl)-7-[4-(2-pyridyl)benzyl] amino-1(2)H-pyrazolo[4,3-d]pyrimidine (**5g**)*

A mixture of 3-isopropyl-5-methylsulfonyl-7-[4-(2-pyridyl) benzyl]amino-1(2)H-pyrazolo[4,3-*d*]pyrimidine (**4**) (0.2 g, 0.47 mmol) and thiomorpholine (3 mL, 29 mmol) in a sealed ampoule was heated at 150 °C for 5 h. Excess thiomorpholine was evaporated at a temperature below 70 °C, and the residue was partitioned between H_2O and $CHCl_3$. The combined organic phase was dried with sodium sulfate and evaporated under vacuum. The product was purified by column chromatography, stepwise (2%, 3%, 4%) with MeOH in $CHCl_3$. Chromatography provided (after evaporation under vacuum) a noncrystalizable, amorphous yellow glass foam, with mass = 0.05 g, and 24% yield. ESI + *m*/*z* 446.1 $[M+H]^+$, ES- *m*/*z* 444.1 $[M-H]^-$. ^1H (500 MHz; $CDCl_3$): 1.33 (d, *J* = 6.72 Hz, 6H, $-CH(CH_3)_2$); 2.55–2.57 (m, 4H, 2× $-CH_2-$); 3.30 (sept., *J* = 6.72 Hz, 1H, $-CH(CH_3)_2$); 4.07–4.09 (m, 4H, 2× $-CH_2-$); 4.64 (bd, *J* = 5.20 Hz, 2H, $-NH-CH_2-$); 7.17–7.20 (m, 1H, ArH); 7.28 (d, *J* = 8.25 Hz, 2H, ArH); 7.60 (d, *J* = 7.95 Hz, 1H, ArH); 7.69 (dt, *J* = 7.95 Hz, *J* = 1.83 Hz, 1H, ArH); 7.79 (d, *J* = 8.25 Hz, 2H, ArH); 8.60–8.62 (m, 1H, ArH). Anal. ($C_{24}H_{27}N_7S$) C, H, N, S.

*4.1.13. 3-Isopropyl-5-[2-(2-hydroxyethyl)piperidin-1-yl]-7-[4-(2-pyridyl)benzyl]amino-1(2)H-pyrazolo[4,3-d]pyrimidine (**5h**)*

A solution of 3-isopropyl-5-methylsulfonyl-7-[4-(2-pyridyl) benzyl]amino-1(2)H-pyrazolo[4,3-*d*]pyrimidine (**4**) (0.20 g, 0.47 mmol) and 2-piperidineethanol (2.3 mL, 19 mmol) was heated in a sealed ampoule at 130 °C for 35 h. Excess amine was evaporated (0.2 torr, 85 °C) and the residue was partitioned between H_2O and dichloromethane. The combined organic phase was dried with sodium sulfate and evaporated under vacuum. The product was purified by column chromatography, stepwise (4%, 6%, 8%) with MeOH in $CHCl_3$. Chromatography provided (after evaporation under vacuum) a noncrystalizable, amorphous colorless glass foam, with mass = 0.022 g, and a 10% yield. ESI + *m*/*z* 472.2 (100%) $[M+H]^+$, 236.7 (90%) $[M+2H]^{2+}$, ESI- *m*/*z* 470.2 $[M-H]^-$.^1H (500 MHz; $CDCl_3$): 1.19 (d, *J* = 6.72 Hz, 6H, $-CH(CH_3)_2$); 1.41–1.44 (m, 1H); 1.55–1.76 (m, 5H); 2.01–2.17 (m, 1H); 2.77 (bt, 1H); 3.06 (sept., *J* = 7.03 Hz, 1H, $-CH(CH_3)_2$); 3.40 (bt, 1H); 3.67–3.69 (bs, 1H); 4.59 (bs, 1H); 4.70–4.76 (m, 3H); 7.16–7.18 (m, 1H, ArH); 7.40 (d, *J* = 7.95 Hz, 2H, ArH); 7.60 (d, *J* = 8.25 Hz, 1H, ArH); 7.68 (td, *J* = 7.95 Hz, *J* = 1.83 Hz, 1H, ArH); 7.81 (d, *J* = 8.25 Hz, 2H, ArH); 8.60–8.61 (m, 1H, ArH). ^{13}C (125 MHz; $CDCl_3$): 19.5, 20.9, 21.6, 25.4, 25.8, 29.6, 29.7, 31.9, 40.1, 44.3, 48.5, 57.8, 120.2, 122.1, 126.9, 128.2, 136.8, 138.2, 139.0, 149.4, 151.3, 156.0, 157.0. Anal. ($C_{27}H_{33}N_7O$) C, H, N.

*4.1.14. 3-Isopropyl-5-(2-aminoethyl)amino-7-[4-(2-pyridyl)benzyl] amino-1(2)H-pyrazolo[4,3-d]pyrimidine (**5i**)*

A solution of 3-isopropyl-5-methylsulfonyl-7-[4-(2-pyridyl) benzyl]amino-1(2)H-pyrazolo[4,3-*d*]pyrimidine (**4**) (0.3 g, 0.71 mmol) and 2-aminoethylamine (10 mL, 150 mmol) in a sealed ampoule was heated at 125 °C for 20 h. Excess amine was evaporated at a temperature below 70 °C, and the residue was partitioned between H_2O and $CHCl_3$. The combined organic phase was dried with sodium sulfate and evaporated under vacuum. The product was purified by column chromatography, stepwise (6%, 8%, 11%, 13%) with MeOH in $CHCl_3$ with a trace of concentrated aqueous NH_4OH. Chromatography provided (after evaporation under vacuum) a noncrystalizable, amorphous colorless glass foam, with mass = 0.16 g, and 56% yield. ESI + *m*/*z* 403.1 $[M+H]^+$, ES- *m*/*z* 401.1 $[M-H]^-$. ^1H (500 MHz; $CDCl_3$): 1.27 (d, *J* = 7.03 Hz, 6H, $-CH(CH_3)_2$); 2.79 (t, *J* = 5.50 Hz, 2H, $-CH_2-$); 3.21 (sept., *J* = 6.72 Hz, 1H, $-CH(CH_3)_2$); 3.39 (bs, 2H, $-CH_2-$); 4.58 (bs, 2H, $-NH-CH_2-$); 5.07 (bs, 1H, $-NH-$); 7.14–7.17 (m, 1H, ArH); 7.23 (d, *J* = 8.25 Hz, 2H, ArH); 7.57 (d, *J* = 7.95 Hz, 1H, ArH); 7.66 (td, *J* = 7.95 Hz, *J* = 1.53 Hz, 1H, ArH); 7.74 (d, *J* = 8.25 Hz, 2H, ArH); 8.58 (d, *J* = 3.97 Hz, 1H, ArH). ^{13}C (125 MHz; $CDCl_3$): 21.7; 25.8; 42.0; 43.8; 44.6; 120.7; 122.2; 127.0; 127.9; 136.9; 138.1; 139.5; 149.4; 152.1; 157.0; 158.6. Anal. ($C_{22}H_{26}N_8$) C, H, N.

*4.1.15. 3-Isopropyl-5-(trans-2-aminocyclohexyl)amino-7-[4-(2-pyridyl)benzyl]amino-1(2)H-pyrazolo[4,3-d]pyrimidine (**5j**)*

A solution of 3-isopropyl-5-methylsulfonyl-7-[4-(2-pyridyl) benzyl]amino-1(2)H-pyrazolo[4,3-*d*]pyrimidine (**4**) (1.4 g, 3.32 mmol) in *trans*-1,2-diaminocyclohexane (30 mL, 68 mmol) was heated in a sealed ampoule at 150 °C for 20 h. Excess amine was evaporated at a temperature below 70 °C, and the residue was partitioned between H_2O and $CHCl_3$. The combined organic phase was dried with sodium sulfate and evaporated under vacuum. The product was purified by column chromatography, stepwise (4%, 8%, 11%, 14%) with MeOH in $CHCl_3$ containing a trace of concentrated aqueous NH_4OH. Chromatography provided (after evaporation under vacuum) a noncrystalizable, amorphous colorless glass foam, with mass = 0.20 g, and 13% yield. ESI + *m*/*z* 457.3 (100%) $[M+H]^+$, 229.1 (50%) $[M+2H]^{2+}$, ESI- *m*/*z* 455.3 $[M-H]^-$.^1H (500 MHz; $CDCl_3$): 1.13–1.20 (m, 4H, $-CH_2-$); 1.25 (bs, 6H, $-CH(CH_3)_2$); 1.57–1.59 (m, 2H, $-CH_2-$); 1.86 (bs, 2H, $-CH_2-$); 2.47 (bs, 1H, $>CHNH_2$); 3.15 (sept., *J* = 6.42 Hz, 1H, $CH(CH_3)_2$); 3.56 (bs, 1H, $-CHNH-$); 4.57 (bs, 2H, $-NH-CH_2-$); 7.13 (dd, *J* = 7.34 Hz, *J* = 4.89 Hz, 1H, ArH); 7.28 (d, *J* = 7.95 Hz, 2H, Ar); 7.53 (d, *J* = 7.95 Hz, 1H, ArH); 7.63 (d, *J* = 7.64 Hz, 1H, ArH); 7.73 (d, *J* = 7.95 Hz, 2H, ArH); 8.58 (d, *J* = 4.58 Hz, 1H, ArH). ^{13}C (125 MHz; $CDCl_3$): 18.3; 21.7; 21.8; 24.7; 25.0; 25.9; 32.5; 34.0; 43.7; 46.0; 56.3; 57.2; 57.9; 120.4; 121.9; 126.8; 127.0; 127.4; 127.7; 136.7; 137.9; 139.6; 149.3; 149.6; 151.8; 156.9; 158.0. Anal. ($C_{26}H_{32}N_8$) C, H, N.

*4.1.16. 3-Isopropyl-5-(3-amino-2-hydroxypropyl)amino-7-[4-(2-pyridyl)benzyl]amino-1(2)H-pyrazolo[4,3-d]pyrimidine (**5k**)*

A mixture of 3-isopropyl-5-methylsulfonyl-7-[4-(2-pyridyl) benzylamino]-1(2)H-pyrazolo[4,3-*d*]pyrimidine (**4**) (0.69 g, 1.64 mmol), 1,3-diamino-2-propanol (10 mL, 95 mmol) and 1-methyl-2-pyrolidone 2 mL was heated at 140 °C for 12 h in a sealed ampoule. Excess amine was evaporated at a temperature below 70 °C, and the residue was partitioned between H_2O and $CHCl_3$. The combined organic phase was dried with sodium sulfate and evaporated under vacuum. The product was purified by column chromatography, stepwise (5%, 8%, 11% 14%) with MeOH in $CHCl_3$ containing a trace of concentrated aqueous NH_4OH. Chromatography provided (after evaporation under vacuum) a noncrystalizable, amorphous colorless glass form, with mass = 0.17 g, and 24% yield. ESI + *m*/*z* 433.1 (100%) $[M+H]^+$, 217.6 (90%) $[M+2H]^{2+}$, ESI- *m*/*z* 431.1 $[M-H]^-$. ^1H (500 MHz; DMSO-d_6): 1.27 (d, *J* = 7.03 Hz, 6H, $-CH(CH_3)_2$); 2.40–2.50 (m, 2H, $-CH_2-$); 3.10–3.20 (m, 2H, $-CH_2-$); 2.28–2.33 (m, 1H, $-CH(OH)-$); 3.45–3.49 (m, 1H, $-CH(CH_3)_2$); 4.69 (bs, 2H, $-NH-CH_2-$); 6.06 (app. bt, 1H, $-NH-CH_2-$); 7.26–7.29 (m, 1H, ArH); 7.44 (d, *J* = 8.25 Hz, 2H, ArH); 7.81 (dt, *J* = 7.64 Hz, *J* = 1.83 Hz, 1H, ArH); 7.87–7.89 (m, 2H, ArH, -NH-); 8.01 (d, *J* = 8.56 Hz, 2H, ArH); 8.59–8.60 (m, 1H). ^{13}C (125 MHz; DMSO-d_6): 22.1, 22.2, 26.2, 43.1, 45.7, 46.0, 72.8, 120.6, 123.0, 126.7, 127.0, 127.8, 128.4, 137.7, 137.9, 140.9, 150.0, 156.3, 158.9. Anal. ($C_{23}H_{28}N_8O$) C, H, N.

*4.1.17. 3-Isopropyl-5-(piperazin-1-yl)-7-[4-(2-pyridyl)benzyl] amino-1(2)H-pyrazolo[4,3-d]pyrimidine (**5l**)*

A solution of 3-isopropyl-5-methylsulfonyl-7-[4-(2-pyridyl) benzyl]amino-1(2)H-pyrazolo[4,3-*d*]pyrimidine (**4**) (0.32 g, 0.76 mmol) in pyrazine (3 mL, 27 mmol) in a sealed ampoule was heated at 150 °C for 6 h. Excess amine was evaporated at a temperature below 70 °C and the residue was partitioned between H_2O

and $CHCl_3$. The combined organic phase was dried with sodium sulfate and evaporated under vacuum. The product was purified by column chromatography, stepwise (2%, 4%, 5%) with MeOH in $CHCl_3$ containing a trace of concentrated aqueous NH_4OH. Chromatography provided (after evaporation under vacuum) a non-crystalizable, amorphous colorless glass foam, with mass = 0.18 g, and 55% yield. ESI + *m/z* 429.1 $[M+H]^+$, ES- *m/z* 427.1 $[M-H]^-$. ^1H (500 MHz; DMSO-d_6): 1.31 (d, *J* = 7.03 Hz, 6H, −CH(C*H*$_3$)$_2$); 2.73–2.75 (m, 4H, 2×−CH$_2$−), 3.17 (sept., J = 7.03 Hz, 1H, C*H*(CH$_3$)$_2$); 3.58–3.60 (m, 4H, 2×−CH$_2$−); 4.71 (d, *J* = 5.20 Hz, 2H, −NH−C*H*$_2$−); 7.29 (ddd, *J* = 7.34 Hz, *J* = 4.89 Hz, *J* = 0.92 Hz, 1H, ArH); 7.48 (d, *J* = 8.25 Hz, 2H, ArH); 7.84 (dt, *J* = 7.49 Hz, *J* = 1.53 Hz, 1H, ArH); 7.91 (d, *J* = 8.25 Hz, 1H, ArH); 8.04 (d, *J* = 7.64 Hz, 2H, ArH); 8.63 (d, *J* = 4.58 Hz, 1H, ArH). Anal. ($C_{24}H_{28}N_8$) C, H, N.

4.1.18. 3-Isopropyl-5-[2-(dimethylamino)ethyl]amino-7-[4-(2-pyridyl)benzyl]amino-1(2)H-pyrazolo[4,3-d]pyrimidine (**5m**)

A solution of 3-isopropyl-5-methylsulfonyl-7-[4-(2-pyridyl) benzyl]amino-1(2)H-pyrazolo[4,3-*d*]pyrimidine (**4**) (0.3 g, 0.71 mmol) and 2-(dimethylamino)ethylamine (3 mL, 27 mmol) in a sealed ampoule was heated at 140 °C for 5 h. Excess amine was evaporated at a temperature below 50 °C, and the residue was partitioned between H_2O and $CHCl_3$. The combined organic phase was dried with sodium sulfate and evaporated under vacuum. The product was purified by column chromatography, stepwise (5%, 10%, 14%) with MeOH in $CHCl_3$ containing a trace of concentrated aqueous NH_4OH. Chromatography provided a noncrystalizable, amorphous colorless glass foam, with mass = 0.06 g, and 20% yield. ESI + *m/z* 431.2 (100%) $[M+H]^+$, 216.1 (30%) $[M+2H]^{2+}$, ESI- *m/z* 429.2 $[M-H]^-$. ^1H (500 MHz; $CDCl_3$): 1.31 (d, J = 7.03 Hz, 6H, −CH(C*H*$_3$)$_2$); 2.23 (s, 6H, (CH$_3$)$_2$N); 2.65 (t, *J* = 7.64 Hz, 2H, −CH$_2$−); 3.20 (t, *J* = 7.34, 2H, −CH$_2$−); 3.27 (kvint.; *J* = 7.03 Hz, 1H, −C*H*(CH$_3$)$_2$); 4.61 (bs, 2H, −NH−C*H*$_2$−); 6.97 (bs, 1H, −N*H*−CH−); 7.14–7.18 (m, 3H, ArH); 7.55 (d, *J* = 8.25 Hz, 1H, ArH); 7.66 (dd, *J* = 7.64 Hz, J = 1.83 Hz, 1H, ArH); 7.69 (d, *J* = 7.95 Hz, 2H, ArH); 8.55 (d, *J* = 3.97 Hz, 1H, ArH). ^{13}C (125 MHz; $CDCl_3$): 21.8; 26.4; 28.1; 44.0; 45.1; 59.1; 120.9; 122.3; 127.1; 128.0; 137.2; 138.2; 139.1; 149.4; 150.7; 157.0; 161.7. Anal. ($C_{24}H_{30}N_8$) C, H, N.

4.1.19. 3-Isopropyl-5-(trans-4-aminocyclohexyl)amino-7-[4-(2-pyridyl)benzyl]amino-1(2)H-pyrazolo[4,3-d]pyrimidine (**5n**)

3-Isopropyl-5-methylsulfonyl-7-[4-(2-pyridyl)benzyl]amino-1(2)H-pyrazolo[4,3-*d*]pyrimidine (**4**) (0.3 g, 0.71 mmol) in melted *trans*-1,4-diaminocyclohexane (5 g, 44 mmol) was heated in a sealed ampoule at 150 °C for 20 h. Excess amine was evaporated at a temperature below 70 °C, and the residue was partitioned between H_2O and $CHCl_3$. The combined organic phase was dried with sodium sulfate and evaporated under vacuum. The product was purified by column chromatography, stepwise (4%, 8%, 11%, 14%) with MeOH in $CHCl_3$ containing a trace of concentrated aqueous NH_4OH. Chromatography provided (after evaporation under vacuum) a noncrystalizable, amorphous colorless glass foam, with mass = 0.06 g, and 19% yield. ESI + *m/z* 457.3 (100%) $[M+H]^+$, 229.1 (50%) $[M+2H]^{2+}$, ESI- *m/z* 455.3 $[M-H]^-$. ^1H (500 MHz; DMSO-d_6): 1.08–1.18 (m, 4H, 2x−CH$_2$−); 1.27 (d, *J* = 7.03 Hz, 6H, −CH(C*H*$_3$)$_2$); 1.71–1.72 (m, 2H, −CH$_2$−); 1.85–1.87 (m, 2H, −CH$_2$−); 2.50–2.52 (m, 1H, −C*H*−NH−); 3.11 (sept., *J* = 7.03 Hz, 1H, −C*H*(CH$_3$)$_2$); 3.54–3.56 (m, 1H, −C*H*−NH−); 4.68 (bd, *J* = 4.58 Hz, 2H, −NH−C*H*$_2$−); 5.69 (bd, *J* = 7.34 Hz, 1H, −N*H*−CH−); 7.26 (m, 1H, ArH); 7.44 (d, *J* = 8.25 Hz, 2H, ArH); 7.79–7.82 (m, 2H, ArH, and −N*H*−); 7.86–7.88 (m, 1H, ArH); 8.00 (d, *J* = 8.25 Hz, 2H, ArH); 8.59–8.60 (m, 1H, ArH). ^{13}C (125 MHz; DMSO-d_6): 22.1; 26.4, 31.8, 34.9, 43.2, 50.0, 50.4, 120.6, 122.9, 127.0, 128.3, 137.7, 137.8, 141.2, 150.0, 156.3, 157.8. Anal. ($C_{26}H_{32}N_8$) C, H, N.

4.1.20. 3-Isopropyl-5-[4-(2-hydroxyethyl)piperazin-1-yl]-7-[4-(2-pyridyl)benzyl]amino-1(2)H-pyrazolo[4,3-d]pyrimidine (**5o**)

A solution of 3-isopropyl-5-methylsulfonyl-7-[4-(2-pyridyl) benzyl]amino-1(2)H-pyrazolo[4,3-*d*]pyrimidine (**4**) (0.21 g, 0.5 mmol) and 2-piperazin-1-ylethanol (3 mL, 23 mmol) in a sealed ampoule was heated at 150 °C for 5 h. The reaction mixture was partitioned between H_2O and $CHCl_3$. The combined organic phase was dried with sodium sulfate and evaporated under vacuum. The product was purified by column chromatography, stepwise (2%, 3%, 4%) with MeOH in $CHCl_3$. Chromatography provided a syrupy product that crystallized from $CHCl_3$, with m.p. = 135–140 °C, mass = 0.035 g, and 15% yield. ESI + *m/z* 473.1 $[M+H]^+$, ES- *m/z* 471.1 $[M-H]^-$. ^1H (500 MHz; $CDCl_3$ + DMSO-d_6): 1.23 (d, *J* = 7.03 Hz, 6H, −CH(C*H*$_3$)$_2$); 2.45–2.46 (m, 6H, 3× −CH$_2$−); 3.14 (sept., *J* = 6.72 Hz, 1H, −C*H*(CH$_3$)$_2$); 3.50–3.52 (m, 2H, −CH$_2$−); 3.67 (m, 4H, 2× −CH$_2$−); 4.60–4.61 (m, 2H, −NH−C*H*$_2$−); 7.05–7.09 (m, 1H, ArH); 7.18 (bs, 1H, −NH−); 7.31–7.32 (m, 2H, ArH); 7.54–7.59 (m, 2H, ArH); 7.78–7.79 (m, 2H, ArH); 8.47–8.48 (m, 1H, ArH); 11.3 (bs, 1H, −NH−). ^{13}C (125 MHz; $CDCl_3$ + DMSO-d_6): 21.6, 26.5, 44.0, 44.6, 52.9, 57.7, 59.8, 120.3, 122.2, 126.9, 128.4, 136.8, 138.3, 140.0, 149.6, 156.7, 157.9. Anal. ($C_{26}H_{32}N_8O$) C, H, N.

4.1.21. 3-Isopropyl-5-(4-methoxybenzyl)amino-7-[4-(2-pyridyl) benzyl]amino-1(2)H-pyrazolo[4,3-d]pyrimidine (**5p**)

A solution of 3-isopropyl-5-methylsulfonyl-7-[4-(2-pyridyl) benzyl]amino-1(2)H-pyrazolo[4,3-*d*]pyrimidine (**4**) (0.5 g, 1.18 mmol) in 4-methoxybenzylamine (10 mL, 58 mmol) was heated in a sealed ampoule at 150 °C for 5 h. Excess amine was evaporated at a temperature below 70 °C, and the residue was partitioned between H_2O and $CHCl_3$. The combined organic phase was dried with sodium sulfate and evaporated under vacuum. The product was purified by column chromatography, stepwise (3%, 5%, 7%) with MeOH in $CHCl_3$. Chromatography provided (after evaporation under vacuum) a noncrystalizable, amorphous colorless glass, with mass = 0.15 g, and 26% yield. ESI + *m/z* 480.3 $[M+H]^+$, ES- *m/z* 478.3 $[M-H]^-$. ^1H (500 MHz; $CDCl_3$): 1.29 (d, *J* = 6.72 Hz, 6H, -CH(C*H*$_3$)$_2$); 3.21 (sept., J = 6.72 Hz, 1H, −C*H*(CH$_3$)$_2$); 3.67 (s, 3H, OCH$_3$); 4.50 (bd, *J* = 3.97 Hz, 2H, −NH−CH$_2$−); 4.69 (bs, 2H, −NH−C*H*$_2$−); 6.72 (d, *J* = 8.56 Hz, 2H, ArH); 7.17–7.22 (m, 3H, ArH, −NH−); 7.29 (d, J = 8.25 Hz, 2H, ArH); 7.59 (d, J = 7.95 Hz, 1H, ArH); 7.69 (dt, J = 7.64 Hz, J = 1.83 Hz, 1H, ArH); 7.78 (d, J = 8.25 Hz, 2H, ArH); 8.60–8.61 (m, 1H, ArH). ^{13}C (125 MHz; $CDCl_3$): 21.8, 26.1, 44.2, 45.4, 55.3, 113.8, 120.7, 122.3, 127.1, 128.1, 128.4, 128.9, 129.0, 137.4, 138.4, 149.6, 157.0, 158.7. Anal. ($C_{28}H_{29}N_7O$) C, H, N.

4.1.22. 3-Isopropyl-5,7-di[4-(2-pyridyl)benzyl]amino-1(2)H-pyrazolo[4,3-d]pyrimidine (**5q**)

A mixture of 3-Isopropyl-5-methylsulfonyl-7-[4-(2-pyridyl) benzyl]amino-1(2)H-pyrazolo[4,3-*d*]pyrimidine (**4**) (0.25 g, 0.59 mmol), 1-[4-(pyridin-2-yl)phenyl]methanamine (0.48 g, 2.6 mmol), ethyldiisopropylamine (0.4 mL, 2.3 mmol) and 1-methyl-2-pyrolidone 1 mL was heated at 150 °C for 5 h in a sealed ampoule. The reaction mixture was concentrated under vacuum and the residue was partitioned between H_2O and $CHCl_3$. The combined organic phase was dried with sodium sulfate. The product was purified by column chromatography, stepwise (4%, 6%, 8%, 10%) with MeOH in $CHCl_3$ containing a trace of concentrated aqueous NH_4OH. Chromatography provided (after evaporation under vacuum) a noncrystalizable, amorphous colorless glass form, with mass = 0.069 g, and 21% yield. ESI + *m/z* 527.3 $[M+H]^+$, ES- *m/z* 525.3 $[M-H]^-$. ^1H (500 MHz; DMSO-d_6): 1.30 (d, *J* = 7.03 Hz, 6H, −CH(C*H*$_3$)$_2$); 3.22–3.27 (m, 1H, −C*H*−(CH$_3$)$_2$); 4.62 (bs, 2H, −NH−C*H*$_2$−); 4.73 (d, *J* = 5.81 Hz, 2H, −NH−C*H*$_2$−); 7.27–7.37 (m, 6H, ArH); 7.74–7.77 (m, 4H, ArH); 7.91–7.93 (m, 4H, ArH); 8.59–8.60 (m, 2H, ArH). Anal. ($C_{32}H_{30}N_8$) C, H, N.

4.1.23. 3-Isopropyl-7-[4-(2-pyridyl)benzyl]amino-1(2)H-pyrazolo [4,3-d]pyrimidine (**6**)

A solution of 7-chloro-3-isopropyl-1(2)H-pyrazolo[4,3-*d*]pyrimidine (Moravcova 2003), 1-[4-(pyridin-2-yl)phenyl]methanamine (0.31 g, 1.58 mmol) and ethyldiisopropylamine (0.4 mL, 2.3 mmol) in $CHCl_3$/t-BuOH (6 mL/1 mL) was heated for 1 h at 60 °C. After cooling to room temperature the reaction mixture was concentrated under vacuum and the residue was partitioned between H_2O and $CHCl_3$. The combined organic phase was dried with magnesim sulfate and evaporated. Column chromatograpy, stepwise (1%, 2%, and 4%) with MeOH in $CHCl_3$ provided (after evaporation under vacuum) a noncrystalizable, amorphous colorless glass form, with mass = 0.442 g, and 81% yield. ESI + *m*/*z* 345.1 $[M+H]^+$, ESI- *m*/*z* 343.1 $[M-H]^-$. ^1H (500 MHz; DMSO-d_6): 1.33 (d, J = 7.03 Hz, 6H, $-CH(CH_3)_2$); 3.29 (m, 1H, $-CH(CH_3)_2$); 4.78 (bs, 2H, $-NH-CH_2-$); 7.27–7.29 (m, 1H, ArH); 7.46 (d, J = 7.03 Hz, 2H, ArH); 7.80–7.83 (m, 1H); 7.87–7.89 (m, 2H, ArH, and −NH−); 8.03 (d, J = 7.03 Hz, 2H, ArH); 8.21 (bs, 1H, ArH, *H*C5); 8.60 (d, J = 4.28 Hz, 1H, ArH); 12.26 (bs, 1H, −NH−). ^{13}C (125 MHz; DMSO-d_6): 22.2, 26.8, 43.6, 120.6, 122.4, 123.0, 126.9, 127.1, 128.5, 128.8, 137.7, 138.1, 139.4, 140.3, 149.6, 150.0, 150.7, 151.2, 156.3. Anal. ($C_{20}H_{20}N_6$) C, H, N.

4.2. Cytotoxicity assays on cancer cell lines

The cytotoxicity of each compound was determined using cell lines of different histological origin, as described earlier [17,36]. Briefly, cells were treated in triplicate with three different doses of each compound for 72 h. After treatments, Calcein AM solution was added, and fluoresence from live cells was measured at 485 nm/538 nm (excitation/emission) using a Fluoroskan Ascent microplate reader (Labsystems). The IC_{50} value, that is, the drug concentration lethal to 50% of the tumor cells, was calculated from the dose response curves that resulted from the assays. MCF-7, K562, G361, and HCT-116 cell lines were maintained in DMEM medium supplemented with 10% fetal bovine serum, penicillin (100 U/ml), and streptomycin (100 μg/ml). All cell lines were cultivated at 37 °C in 5% CO_2.

4.3. Kinase inhibition assays

CDK2/Cyclin E kinase was produced in Sf9 insect cells via baculoviral infection and purified on a NiNTA column (Qiagen). Other CDKs were purchased from ProQinase GmbH. Kinase reactions of each test compound were assayed using a mixture of the following: 1 mg/mL histone H1 (for CDK2 and CDK5), 15 μM and 0.15 μM ATP for CDK2 and CDK5, respectively; 0.05 μCi [γ-^{33}P]ATP; the test compound; and reaction buffer, in a final volume of 10 μL. The reaction buffer consisted of: 60 mM HEPES-NaOH, pH 7.5, 3 mM $MgCl_2$, 3 mM $MnCl_2$, 3 μM Na-orthovanadate, 1.2 mM DTT, and 2.5 μg/50 μl $PEG_{20.000}$). The reactions were stopped by adding 5 μL of 3% aqueous H_3PO_4. Aliquots were spotted onto P-81 phosphocellulose (Whatman), washed 3 times with 0.5% aqueous H_3PO_4, and finally air-dried. Kinase inhibition was quantified using a FLA-7000 digital image analyzer (Fujifilm) [17,36]. The concentration of each test compound required to decrease CDK activity by 50% was determined from its dose-response curve and designated as its IC_{50}.

4.4. Immunoblotting and antibodies

Immunoblotting was performed as previously described [17,36]. Briefly, cell lysates were prepared by harvesting cells in Laemmli sample buffer. Proteins were separated on SDS-polyacrylamide gels and electroblotted onto nitrocellulose membranes. After blocking, the membranes were incubated with specific primary antibodies overnight, washed, and then incubated with peroxidase-conjugated secondary antibodies. Finally, peroxidase activity was detected with ECL + reagents (AP Biotech) using a CCD camera LAS-4000 (Fujifilm). Specific antibodies were purchased from: Cell Signaling (anti-FAK), Santa Cruz Biotechnology (anti-PARP, clone F-2; anti-β-actin, clone C4; anti-Mcl-1, clone S-19), Bethyl Laboratories (anti-pRNA polymerase II antibodies phosphorylated at S5 and S2), Millipore (anti-RNA polymerase II, clone ARNA-3), Roche Applied Science (anti-5-bromo-2′-deoxyuridine-fluorescein, clone BMC 9318), Sigma-Aldrich (anti-α-tubulin, clone DM1A), Thermofisher Scientific (anti-pFAK, S732), Bioss (anti-CDK5); or were generously gifted by Dr. B. Vojtěšek (anti-p53, clone DO-1).

4.5. Caspase activity assay

The cells were homogenized on ice for 20 min in an extraction buffer (10 mM KCl, 5 mM HEPES, 1 mM EDTA, 1 mM EGTA, 0.2% CHAPS, inhibitors of proteases, pH 7.4). The homogenates were clarified by centrifugation at 10,000 × g for 30 min at 4 °C, and then the proteins were quantified and diluted to equal concentrations. Lysates were then incubated for 3 h with 100 μM Ac-DEVD-AMC, a substrate of caspases 3 and 7, in assay buffer (25 mM PIPES, 2 mM EGTA, 2 mM $MgCl_2$, 5 mM DTT, pH 7.3). The fluorescence of the product was measured using a Fluoroskan Ascent microplate reader (Labsystems) at 355/460 nm (excitation/emission).

4.6. Cell cycle analysis

Sub-confluent cells were treated with different concentrations of each test compound for 24 h. The cultures were pulse-labeled with 10 μM 5-bromo-2′-deoxyuridine (BrdU) for 30 min at 37 °C prior to harvesting. The cells were then washed in PBS, fixed with 70% ethanol, and denatured in 2 M HCl. Following neutralization, the cells were stained with anti-BrdU fluorescein-labeled antibodies, washed, stained with propidium iodide, and analyzed by flow cytometry using a 488 nm laser (Cell Lab Quanta SC, Beckman Coulter) [17,36].

Acknowledgment

The authors gratefully acknowledge support from the Ministry of Education, Youth and Sports of the Czech Republic (the National Program of Sustainability I—Grant LO1204), and from the Czech Science Foundation (15-15264S and 15-17282Y).

Appendix A. Supplementary data

Supplementary data related to this article can be found at http://dx.doi.org/10.1016/j.ejmech.2016.01.011.

References

[1] M. Malumbres, Cyclin-dependent kinases, Genome Biol. 15 (2014) 122.
[2] U. Asghar, A.K. Witkiewicz, N.C. Turner, E.S. Knudsen, The history and future of targeting cyclin-dependent kinases in cancer therapy, Nat. Rev. Drug Discov. 14 (2015) 130–146.
[3] S.J. McClue, D. Blake, R. Clarke, A. Cowan, L. Cummings, P.M. Fischer, M. MacKenzie, J. Melville, K. Stewart, S. Wang, N. Zhelev, D. Zheleva, D.P. Lane, In vitro and in vivo antitumor properties of the cyclin dependent kinase inhibitor CYC202 (R-roscovitine), Int. J. Cancer 102 (2002) 463–468.
[4] H.H. Sedlacek, Mechanisms of action of flavopiridol, Crit. Rev. Oncol. Hematol. 38 (2001) 139–170.
[5] D.W. Fry, P.J. Harvey, P.R. Keller, W.L. Elliott, M. Meade, E. Trachet, M. Albassam, X. Zheng, W.R. Leopold, N.K. Pryer, P.L. Toogood, Specific inhibition of cyclin-dependent kinase 4/6 by PD 0332991 and associated antitumor activity in human tumor xenografts, Mol. Cancer Ther. 3 (2004) 1427–1438.

[6] N. Kwiatkowski, T. Zhang, P.B. Rahl, B.J. Abraham, J. Reddy, S.B. Ficarro, A. Dastur, A. Amzallag, S. Ramaswamy, B. Tesar, C.E. Jenkins, N.M. Hannett, D. McMillin, T. Sanda, T. Sim, N.D. Kim, T. Look, C.S. Mitsiades, A.P. Weng, J.R. Brown, C.H. Benes, J.A. Marto, R.A. Young, N.S. Gray, Targeting transcription regulation in cancer with a covalent CDK7 inhibitor, Nature 511 (2014) 616–620.
[7] T.K. Albert, C. Rigault, J. Eickhoff, K. Baumgart, C. Antrecht, B. Klebl, G. Mittler, M. Meisterernst, Characterization of molecular and cellular functions of the cyclin-dependent kinase CDK9 using a novel specific inhibitor, Br. J. Pharmacol. 171 (2014) 55–68.
[8] S. Dhillon, Palbociclib: first global approval, Drugs 75 (2015) 543–551.
[9] A. DeMichele, A.S. Clark, K.S. Tan, D.F. Heitjan, K. Gramlich, M. Gallagher, P. Lal, M. Feldman, P. Zhang, C. Colameco, D. Lewis, M. Langer, N. Goodman, S. Domchek, K. Gogineni, M. Rosen, K. Fox, P. O'Dwyer, CDK 4/6 inhibitor palbociclib (PD0332991) in Rb+ advanced breast cancer: phase II activity, safety, and predictive biomarker assessment, Clin. Cancer Res. 21 (2015) 995–1001.
[10] R.S. Finn, J.P. Crown, I. Lang, K. Boer, I.M. Bondarenko, S.O. Kulyk, J. Ettl, R. Patel, T. Pinter, M. Schmidt, Y. Shparyk, A.R. Thummala, N.L. Voytko, C. Fowst, X. Huang, S.T. Kim, S. Randolph, D.J. Slamon, The cyclin-dependent kinase 4/6 inhibitor palbociclib in combination with letrozole versus letrozole alone as first-line treatment of oestrogen receptor-positive, HER2-negative, advanced breast cancer (PALOMA-1/TRIO-18): a randomised phase 2 study, Lancet Oncol. 16 (2015) 25–35.
[11] R. Jorda, K. Paruch, V. Krystof, Cyclin-dependent kinase inhibitors inspired by roscovitine: purine bioisosteres, Curr. Pharm. Des. 18 (2012) 2974–2980.
[12] R. Jorda, L. Havlicek, I.W. McNae, M.D. Walkinshaw, J. Voller, A. Sturc, J. Navratilova, M. Kuzma, M. Mistrik, J. Bartek, M. Strnad, V. Krystof, Pyrazolo [4,3-*d*]pyrimidine bioisostere of roscovitine: evaluation of a novel selective inhibitor of cyclin-dependent kinases with antiproliferative activity, J. Med. Chem. 54 (2011) 2980–2993.
[13] E. Reznickova, S. Weitensteiner, L. Havlicek, R. Jorda, T. Gucky, K. Berka, V. Bazgier, S. Zahler, V. Krystof, M. Strnad, Characterization of a pyrazolo[4,3-*d*]pyrimidine inhibitor of cyclin-dependent kinases 2 and 5 and aurora A with pro-apoptotic and anti-angiogenic activity in vitro, Chem. Biol. Drug Des. 85 (2015) 1528–1540.
[14] I.M. Sroka, E.H. Heiss, L. Havlicek, F. Totzke, Y. Aristei, P. Pechan, M.H. Kubbutat, M. Strnad, V.M. Dirsch, A novel roscovitine derivative potently induces G1-phase arrest in platelet-derived growth factor-BB-activated vascular smooth muscle cells, Mol. Pharmacol. 77 (2010) 255–261.
[15] S.B. Weitensteiner, J. Liebl, V. Krystof, L. Havlicek, T. Gucky, M. Strnad, R. Furst, A.M. Vollmar, S. Zahler, Trisubstituted pyrazolopyrimidines as novel angiogenesis inhibitors, PLoS One 8 (2013) e54607.
[16] K. Bettayeb, N. Oumata, A. Echalier, Y. Ferandin, J.A. Endicott, H. Galons, L. Meijer, CR8, a potent and selective, roscovitine-derived inhibitor of cyclin-dependent kinases, Oncogene 27 (2008) 5797–5807.
[17] T. Gucky, R. Jorda, M. Zatloukal, V. Bazgier, K. Berka, E. Reznickova, T. Beres, M. Strnad, V. Krystof, A novel series of highly potent 2,6,9-trisubstituted purine cyclin-dependent kinase inhibitors, J. Med. Chem. 56 (2013) 6234–6247.
[18] M.P. Trova, K.D. Barnes, L. Alicea, T. Benanti, M. Bielaska, J. Bilotta, B. Bliss, T.N. Duong, S. Haydar, R.J. Herr, Y. Hui, M. Johnson, J.M. Lehman, D. Peace, M. Rainka, P. Snider, S. Salamone, S. Tregay, X. Zheng, T.D. Friedrich, Heterobiaryl purine derivatives as potent antiproliferative agents: inhibitors of cyclin dependent kinases. Part II, Bioorg. Med. Chem. Lett. 19 (2009) 6613–6617.
[19] M.P. Trova, K.D. Barnes, C. Barford, T. Benanti, M. Bielaska, L. Burry, J.M. Lehman, C. Murphy, H. O'Grady, D. Peace, S. Salamone, J. Smith, P. Snider, J. Toporowski, S. Tregay, A. Wilson, M. Wyle, X. Zheng, T.D. Friedrich, Biaryl purine derivatives as potent antiproliferative agents: inhibitors of cyclin dependent kinases. Part I, Bioorg. Med. Chem. Lett. 19 (2009) 6608–6612.
[20] D. Parry, T. Guzi, F. Shanahan, N. Davis, D. Prabhavalkar, D. Wiswell, W. Seghezzi, K. Paruch, M.P. Dwyer, R. Doll, A. Nomeir, W. Windsor, T. Fischmann, Y. Wang, M. Oft, T. Chen, P. Kirschmeier, E.M. Lees, Dinaciclib (SCH 727965), a novel and potent cyclin-dependent kinase inhibitor, Mol. Cancer Ther. 9 (2010) 2344–2353.
[21] D. Moravcova, L. Havlicek, V. Krystof, R. Lenobel, M. Strnad, Novel pyrazolo [4,3-*d*]pyrimidines, processes for their preparation and method for therapy. WO 2003/082872, 2003.
[22] K. Bettayeb, H. Sallam, Y. Ferandin, F. Popowycz, G. Fournet, M. Hassan, A. Echalier, P. Bernard, J. Endicott, B. Joseph, L. Meijer, N-&-N, a new class of cell death-inducing kinase inhibitors derived from the purine roscovitine, Mol. Cancer Ther. 7 (2008) 2713–2724.
[23] Y.T. Chang, N.S. Gray, G.R. Rosania, D.P. Sutherlin, S. Kwon, T.C. Norman, R. Sarohia, M. Leost, L. Meijer, P.G. Schultz, Synthesis and application of functionally diverse 2,6,9-trisubstituted purine libraries as CDK inhibitors, Chem. Biol. 6 (1999) 361–375.
[24] L. Havlicek, J. Hanus, J. Vesely, S. LeClerc, L. Meijer, G. Shaw, M. Strnad, Cytokinin-derived cyclin-dependent kinase inhibitors: synthesis and cdc2 inhibitory activity of olomoucine and related compounds, J. Med. Chem. 40 (1997) 408–412.
[25] N. Oumata, K. Bettayeb, Y. Ferandin, L. Demange, A. Lopez-Giral, M.L. Goddard, V. Myrianthopoulos, E. Mikros, M. Flajolet, P. Greengard, L. Meijer, H. Galons, Roscovitine-derived, dual-specificity inhibitors of cyclin-dependent kinases and casein kinases 1, J. Med. Chem. 51 (2008) 5229–5242.
[26] B.A. Carlson, M.M. Dubay, E.A. Sausville, L. Brizuela, P.J. Worland, Flavopiridol induces G1 arrest with inhibition of cyclin-dependent kinase (CDK) 2 and CDK4 in human breast carcinoma cells, Cancer Res. 56 (1996) 2973–2978.
[27] R. Chen, W.G. Wierda, S. Chubb, R.E. Hawtin, J.A. Fox, M.J. Keating, V. Gandhi, W. Plunkett, Mechanism of action of SNS-032, a novel cyclin-dependent kinase inhibitor, in chronic lymphocytic leukemia, Blood 113 (2009) 4637–4645.
[28] S.R. Whittaker, M.I. Walton, M.D. Garrett, P. Workman, The Cyclin-dependent kinase inhibitor CYC202 (R-roscovitine) inhibits retinoblastoma protein phosphorylation, causes loss of Cyclin D1, and activates the mitogen-activated protein kinase pathway, Cancer Res. 64 (2004) 262–272.
[29] M. Daval, T. Gurlo, S. Costes, C.J. Huang, P.C. Butler, Cyclin-dependent kinase 5 promotes pancreatic beta-cell survival via Fak-Akt signaling pathways, Diabetes 60 (2011) 1186–1197.
[30] Q. Liang, L. Li, J. Zhang, Y. Lei, L. Wang, D.X. Liu, J. Feng, P. Hou, R. Yao, Y. Zhang, B. Huang, J. Lu, CDK5 is essential for TGF-beta1-induced epithelial-mesenchymal transition and breast cancer progression, Sci. Rep. 3 (2013) 2932.
[31] O. Tetsu, F. McCormick, Proliferation of cancer cells despite CDK2 inhibition, Cancer Cell. 3 (2003) 233–245.
[32] J. Du, H.R. Widlund, M.A. Horstmann, S. Ramaswamy, K. Ross, W.E. Huber, E.K. Nishimura, T.R. Golub, D.E. Fisher, Critical role of CDK2 for melanoma growth linked to its melanocyte-specific transcriptional regulation by MITF, Cancer Cell. 6 (2004) 565–576.
[33] C. Abdullah, X. Wang, D. Becker, Expression analysis and molecular targeting of cyclin-dependent kinases in advanced melanoma, Cell Cycle 10 (2011) 977–988.
[34] B.M. Desai, J. Villanueva, T.T. Nguyen, M. Lioni, M. Xiao, J. Kong, C. Krepler, A. Vultur, K.T. Flaherty, K.L. Nathanson, K.S. Smalley, M. Herlyn, The anti-melanoma activity of dinaciclib, a cyclin-dependent kinase inhibitor, is dependent on p53 signaling, PLoS One 8 (2013) e59588.
[35] S. Mohapatra, D. Coppola, A.I. Riker, W.J. Pledger, Roscovitine inhibits differentiation and invasion in a three-dimensional skin reconstruction model of metastatic melanoma, Mol. Cancer Res. 5 (2007) 145–151.
[36] C.B. Baltus, R. Jorda, C. Marot, K. Berka, V. Bazgier, V. Kryštof, G. Prié, M.C. Viaud-Massuard, Synthesis, biological evaluation and molecular modeling of a novel series of 7-azaindole based tri-heterocyclic compounds as potent CDK2/Cyclin E inhibitors, Eur. J. Med. Chem. 108 (2016) 701–719.